

Experimental assessment of the liquefaction resistance of calcareous biogenous sands

Eimar A. Sandoval¹ and Miguel A. Pando²

¹ Assistant Professor, School of Civil Engineering and Geomatics, University of Valle, Cali, Colombia. E-mail: eimar.sandoval@correounivalle.edu.co.

² Associate Professor, Civil and Environmental Engineering Department, University of North Carolina at Charlotte, NC, USA 28233. E-mail: mpando@uncc.edu.

ABSTRACT

Liquefaction is a phenomenon in which soils, typically sands, suddenly lose a substantial amount of their shear strength and stiffness, this often triggered by large-magnitude earthquakes. Most liquefaction research has focused on silicate-based sands and not on other sand types, such as calcareous biogenous sands. Calcareous sands are usually composed of skeletal or non-skeletal remains of marine organisms, with unique characteristics in terms of their mineralogy surface roughness, particle shape, crushability, and intraparticle porosity. The unique characteristics of calcareous sands suggest that their geotechnical engineering behaviour can be substantially different compared to that of terrigenous sands, including their behaviour under seismic loading, which have not been very well studied.

This paper presents the results of an experimental programme aimed at studying the cyclic liquefaction resistance of uncemented calcareous biogenous sands retrieved from south-western Puerto Rico. Evaluation of liquefaction potential involved a comprehensive set of isotropically consolidated undrained cyclic triaxial tests on reconstituted samples of this calcareous sand. The programme also included tests on Ottawa terrigenous silica sand samples prepared and tested in similar conditions for comparison purposes.

In general, the experimental results showed that Cabo Rojo calcareous sands had higher liquefaction resistance compared to Ottawa silica sands tested under similar conditions. Important differences between calcareous and silica sands regarding pore pressure generation characteristics and axial strain accumulation were also observed.

Keywords: calcareous sands, liquefaction resistance, cyclic pore pressure, cyclic axial strain.

RESUMEN

La licuación es un fenómeno en el cual los suelos, típicamente arenas, pierden una cantidad importante de su rigidez y resistencia al esfuerzo cortante, generalmente por causa de sismos de gran magnitud. La mayoría de investigaciones sobre licuación se han enfocado en arenas terrígenas con base de sílice o cuarzo, y no sobre otro tipo de arenas, como las arenas calcáreas biogénicas. Las arenas calcáreas están usualmente compuestas por residuos de organismos marinos esqueléticos y no esqueléticos, con características específicas en términos de su mineralogía, rugosidad superficial, forma de partículas, susceptibilidad al rompimiento y porosidad interna de los granos. Las características particulares de las arenas calcáreas, hacen suponer que su comportamiento ingenieril geotécnico puede ser considerablemente diferente comparado con el de arenas terrígenas, incluyendo su comportamiento bajo carga sísmica, el cual no ha sido estudiado en detalle.

Este artículo presenta los resultados de un programa experimental desarrollado con el fin de estudiar la resistencia a licuación cíclica de una arena calcárea biogénica no cementada, extraída del suroeste de Puerto Rico. La evaluación del potencial de licuación incluyó una extensa cantidad de ensayos triaxiales cíclicos no drenados consolidados isotrópicamente, sobre muestras no cementadas de esta arena calcárea. Para fines de comparación, el programa también incluyó ensayos sobre la arena terrígena de Ottawa bajo condiciones de prueba similares.

En general, los resultados experimentales mostraron que las arenas calcáreas de Cabo Rojo tuvieron mayor resistencia a licuación, comparada con las arenas de Ottawa para condiciones de prueba similares. También se observaron diferencias importantes en cuanto a las características de generación de presiones de poros y acumulación de deformaciones axiales.

Palabras claves: arenas calcáreas, deformación axial cíclica, presión de poros cíclica, resistencia a licuación

Record

Manuscript received: 15/11/2011

Accepted for publications: 25/05/2012

Introduction

Liquefaction is a serious phenomenon which often manifests itself in areas having loose, saturated, sandy soils following strong earthquakes or vibrations. Liquefaction is manifested as a drastic loss of shear strength and stiffness of the affected soil, resulting from a sharp increase in internal pore water pressure which builds up during load cycles imparted by earthquakes or vibrations. If excess pore pressures increase enough, the soil may lose all its strength and rigidity, leading eventually to behaviour similar to that of liquid, hence the term liquefaction. Due to soil liquefaction, there may be ground subsidence and settlements, sand boils, lateral spreading, slope failures and damage or even collapse of structures.

The significance of damage which can be caused by liquefaction has been recognised for many years (e.g. Yoshimi *et al.*, 1977; Seed, 1979; Seed & Idriss, 1982). The 1964 earthquakes in Alaska, U.S.A. and Niigata, Japan, represent two major seismic events where extensive damage was reported due to liquefaction thereby highlighting its importance. Extensive work has been carried out worldwide since these two earthquakes to better understand soil liquefaction. Progress in this area has been periodically summarised in state-of-the-art reports and monographs such as that published by the Earthquake Engineering Research Institute (EERI) (Seed & Idriss, 1982), the proceedings of a workshop run by the US National Research Council (NRC, 1985), the US National Center for Earthquake Engineering Research (NCEER) (Youd *et al.*, 2001) and a very recent monograph by Idriss & Boulanger (2010). Even though much progress has been made in understanding the complexity of the phenomenon, many aspects still lack important knowledge requiring ongoing research. Most engineering procedures for assessing soil liquefaction potential have been based on field data gathered over the years from sites providing evidence of liquefaction (i.e. empirical). Most case histories used in developing such empirical liquefaction screening methods have been based on sites where liquefied deposits have primarily consisted of silica sands.

The following section provides background information regarding one of the most commonly-used empirical procedures for assessing liquefaction potential based on the geotechnical standard penetration test (SPT) field test. Besides providing valuable background information for readers new to the subject, the material also shows that the empirical methods used in practice are mostly based on liquefaction case histories involving silicate-based terrigenous sandy soil deposits (i.e. transported from land) containing mineral grains such as quartz and feldspar. There is thus an important gap in current knowledge as few or no liquefaction case

histories involving marine biogenous calcareous sands (uncemented or cemented) have been included in current liquefaction case history databases (e.g. Idriss & Boulanger, 2010). This paper is focused on calcareous biogenous marine sands, thus hopes to motivate research on non-silica sand liquefaction and to assess the influence of factors such as origin, genesis, deposition history, and mineralogy.

It presents a summary of results from an experimental research programme aimed at studying the liquefaction resistance of calcareous sands retrieved from surficial beach deposits at Cabo Rojo, south-western Puerto Rico. The experimental programme involved mineralogical and grain characterisation, critical state line (CSL) evaluation, and 31 undrained cyclic triaxial tests on isotropically-consolidated reconstituted samples of uncemented calcareous sands. The triaxial samples were tested at three relative densities and three isotropic consolidation stress levels. The experimental programme included similar tests carried out on Ottawa terrigenous silica sand samples for comparison purposes; these were prepared using similar techniques and tested under the same experimental conditions.

Background

SPT-based simplified liquefaction evaluation methodology

This section provides background on how liquefaction potential of sandy deposits is commonly assessed in practice. The methodology presented was based on an extensive database of case histories of sites where evidence of cyclic liquefaction has been reported following a major earthquake. This methodology is based on classical work by Seed & Idriss (1971) and multiples updates including the recent work by Idriss & Boulanger (2010).

The field data regarding each case history in the SPT-based liquefaction database has been interpreted and analysed to assess the cyclic stresses levels which would induce cyclic liquefaction. For the SPT-based methodology, these interpreted cyclic stresses levels were compared to field SPT blow counts. Figure 1 gives a typical graph summarising empirical data from the SPT-based liquefaction case history database. This plot shows normalised cyclic stresses (presented as cyclic stress ratio - CSR) compared to corresponding normalised SPT blow counts ($N_{1,60}$). The solid circles represent points where cyclic liquefaction occurred and the open circles the data points where no liquefaction was observed. The solid black line represents an empirically based line that can be used to estimate the cyclic stresses that would trigger cyclic liquefaction for a certain SPT blow count. Several versions of this curve have been presented over the years, changing as the SPT-based cyclic liquefaction database gains additional case histories. Versions of this line also differ based on differences in case history interpretations.

Existing procedures for estimating liquefaction potential are currently based on empirical data gathered from sites primarily involving silica sandy soils; a review of the relevant liquefaction literature did not reveal a specific procedure for sandy soil having other mineralogy types or origins such as the calcareous sands investigated in this article.

The definition of liquefaction used in this study

As mentioned earlier, soil liquefaction is a complex phenomenon, involving different soil responses depending on the material stress-strain behaviour, type of loading, initial stress, etc.

For the purposes of this paper, liquefaction refers to “cyclic liquefaction” involving cyclic softening of the soil due to cyclic loading (e.g. earthquake loading) having sufficient intensity (i.e. cyclic stress levels and/or duration) to allow enough build up of excess pore pressures to make the sandy soil reach a state of zero effective stress (Robertson, 1994). Robertson & Wride (1998) have provided a definition for different types of liquefaction, including cyclic liquefaction. Most liquefaction research, including the SPT-based simplified method presented above, has been re-

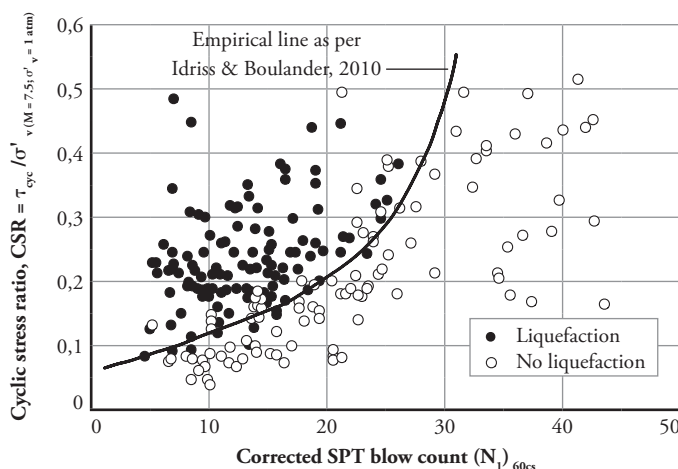


Figure 1. An example of the SPT-based database used for estimating liquefaction resistance (CRR) for silica-based sand deposits (Adapted from Idriss & Boulanger, 2010)

lated to cyclic liquefaction. Cyclic liquefaction usually applies to level or gently sloping ground where shear stress reversal occurs during earthquake loading (Robertson & Wride, 1998; Pando & Robertson, 1995).

Marine biogenous sediments and calcareous sands

Marine biogenous sediments may be siliceous or calcareous and are formed from planktonic organisms, the most abundant organisms in the ocean. Phytoplankton (having plant-like photosynthesis) and zooplankton (grazing like animals) are the two main types of plankton. The insoluble shells of these creatures can be formed of calcite or silica. Calcareous biogenous sediments (the focus of this paper) consist of large accumulations of the skeletal remains of plants and animal life. Skeletal grains are formed as internal or external skeletal units of marine organisms, including crustose and articulate corallines, mollusc shells, forams, gastropods, algae, and echinoid fragments. The calcium carbonate content in skeletal grains is primarily determined by the marine organism from which the grains were derived, in turn, being dependent on local water temperatures and nutrient availability and type (Morelock & Ramirez, 2004). The most common biogenic calcareous particles are shells of foraminifera-micro-organisms, usually being less than 1 mm in diameter (Silva, 1974). Calcite is the main component of calcareous sand (usually greater than 90% calcium carbonate content).

Calcareous sands are unique in terms of particle characteristics, including mineralogy, shape, surface texture, high void ratio, and intra-porosity. Calcareous sands have variable cementation, ranging from non-cemented to strongly-cemented state. These sands are more crushable, more contractive, and less stiff than terrigenous silica sands due to their unique particle properties and carbonate content (Cataño & Pando, 2010).

Methodology

The experimental programme used in this study primarily involved sand mineralogical and grain characterisation, characterising the CSL and consolidated undrained cyclic triaxial testing of specimens prepared using Cabo Rojo calcareous sands and Ottawa silica sands. Thirty-nine consolidated undrained cyclic triaxial tests were performed: 31 of them on Cabo Rojo calcareous sands and 8 on Ottawa silica sands.

Description of test sand materials used

The calcareous sand being studied was collected from a beach in Puerto Real, Cabo Rojo, south-western Puerto Rico; it was retrieved from the near surface beach using an ordinary shovel and buckets. This sand was uncemented and classified as being white to yellow, fine- to medium-grained, poorly-graded, having sub-angular to angular grains and high internal po-

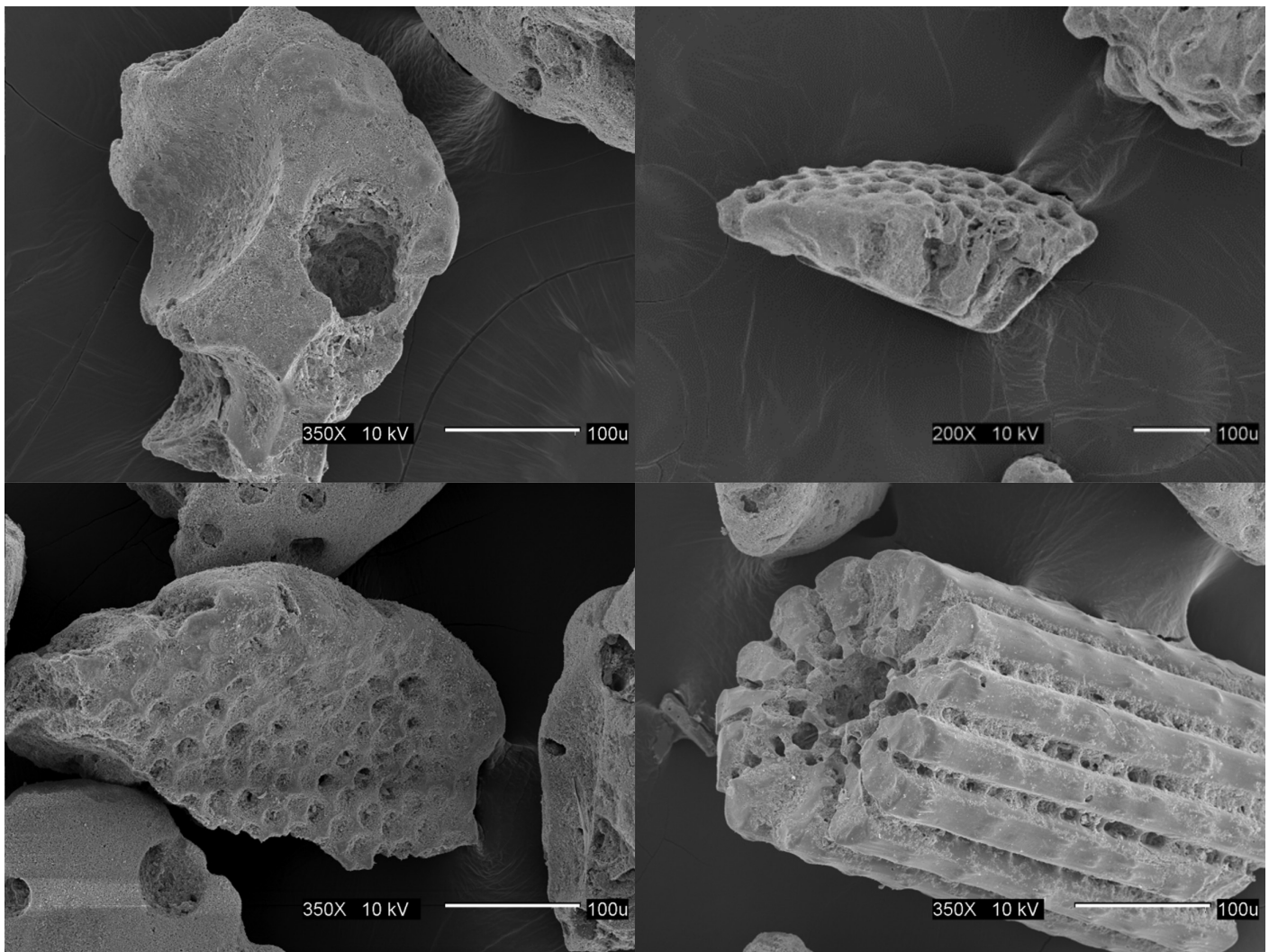


Figure 2. Micrographs of Cabo Rojo uncemented calcareous sand.

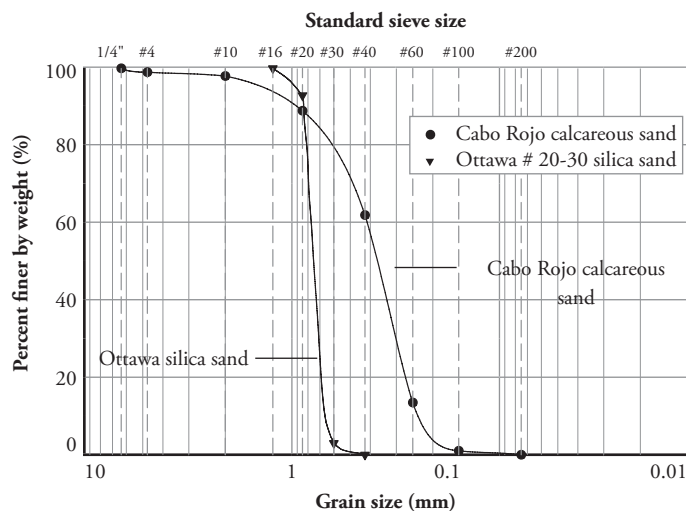
Table 1. Summary of index properties for both sands tested.

Parameter	Cabo rojo calcareous	Ottawa silica sand	ASTM standard
D_{10} (mm)	0.24	0.65	ASTM D422-463
D_{30} (mm)	0.30	0.71	
D_{50} (mm)	0.37	0.75	
D_{60} (mm)	0.41	0.78	
C_u	1.75	2.1	
C_c	0.94	1.1	
G_s	2.84	2.65	ASTM D854
γ_{min} (kN/m ³)	9.10	14.6	ASTM D4254
e_{max}	2.07	0.78	
γ_{max} (kN/m ³)	11.1	17.3	Alternative method
e_{min}	1.51	0.50	

rosity (Figure 2 shows grain characteristics for this sand). This calcareous sand had at least 91% calcium carbonate content. Ottawa silica sand was also tested; this is white, fine- to medium-grained, poorly-graded, having rounded grains and is a terrigenous quartzitic sand having no calcium carbonate content. Table 1 lists the main index properties for both test sands and Figure 3 shows their grain size distribution. Besides having different mineralogy, these two sands also have important differences in terms of grain characteristics and particle size distribution. For example, Table 1 shows that silica sand is coarser than calcareous sand and its specific gravity is lower.

Cabo Rojo calcareous grain characteristics

Cabo Rojo calcareous sands are sedimentary carbonates for which diagenesis and resulting grain mineralogy are influenced by the depth and temperature of the water column (Morse & Mackenzie 1990, Chaney *et al.* 1982, Morelock & Ramirez 2004). Carbonates are usually dominated by aragonite in shallow waters, followed by magnesium-rich calcites, whereas in deep waters carbonates are composed of calcite having low magnesium content.

**Figure 3.** Grain size distribution curves for both sands tested in this study.

A unique characteristic of calcareous sands is their intra-particle void structure which, combined with the skeletal void ratio, can result in total void ratios being quite higher than void ratios for silica sands. For example, e_{max} and e_{min} values listed in Table 1 were found to be 2.07, 1.51 and 0.78, 0.50 for the calcareous and silica sands respectively. Cabo Rojo sands void ratio values are almost 300% higher than Ottawa sands. Furthermore, due to their mineralogical composition, calcareous sands can have considerably higher specific gravity values than typical values for terrigenous silica sands (≈ 2.65). Cabo Rojo calcareous sands had an average specific gravity value of 2.84. This higher specific gravity value is associated to the unique biogenic characteristics of these sands, and to their mineralogical composition which usually includes heavier minerals than quartz such as calcite and aragonite.

The crushing susceptibility of the Cabo Rojo calcareous sand grains during cyclic triaxial testing was checked by comparing gradation curves before and after selected cyclic triaxial tests. Crushing potential was found to be very low to low, at least for the range of isotropic effective consolidation stresses considered, ranging from 50 to 200 kPa. Cataño & Pando (2010) have also reported low to moderate particle crushability for monotonic isotropic consolidated undrained triaxial compression tests and torsional resonant column tests, including tests with up to 500 kPa effective isotropic consolidation stress. Crushing potential values for the Cabo Rojo calcareous sand experiments reported here thus indicated little to no particle crushing. As mentioned earlier, Cabo Rojo sands were extracted in an uncemented state and then reconstituted in the laboratory without cementation.

Critical state line evaluation of Cabo Rojo calcareous sands

Sands under shear loading may be contractile or dilatant, based on their initial state regarding CSL. The initial state of a sand sample is usually defined in terms of its initial void ratio (e) and effective stress level, such as the effective minor principal stress (σ'_3) or the effective mean principal stress (p'). This initial state is important for liquefaction susceptibility analysis because samples above or to the right of the CSL have a contractile behaviour where the skeleton of particles would tend to compress, and thus develop positive excess pore pressures which would make the sand more susceptible to undergoing cyclic liquefaction. By contrast, sand samples having an initial state below or to the left of the CSL will have a dilatant behaviour according to critical soil mechanics, and will not develop large positive excess pore pressure which would make them less susceptible to cyclic liquefaction. Many authors have proposed parameter variables for quantifying liquefaction potential of sandy soils based on the position of their initial state regarding the CSL. For example, Been & Jefferies (1985) proposed using state parameter Y defined as the difference between the initial void ratio of the sandy soil sample and the void ratio at the CSL for the same effective mean pressure p' . A positive state parameter value would thus represent an initial state of the sandy soil sample on the contractile side of the CSL line, while a negative value would represent a dilatant initial state.

Part of this study involved characterising the CSL for the Cabo Rojo calcareous sands (Figure 4). The lower portion of the CSL was obtained from monotonic isotropically-consolidated undrained (CIU) triaxial compression tests reported by Cataño & Pando (2010). The upper portion of the CSL was obtained as part of this research using the simplified method proposed by Santamarina & Cho (2001).

Figure 4 also shows the average position for the eight groups of calcareous sand samples from Cabo Rojo regarding the CSL. Each group corresponded to the same effective consolidation stress and relative density after consolidation, just before the undrained cyclic loading phase. Figure 4 shows that six of the eight groups of samples were located above the CSL, i.e. on the contractile side, therefore expected to exhibit a higher liquefaction potential compared to the two other groups of samples located below the CSL line (i.e. expected dilatant behaviour).

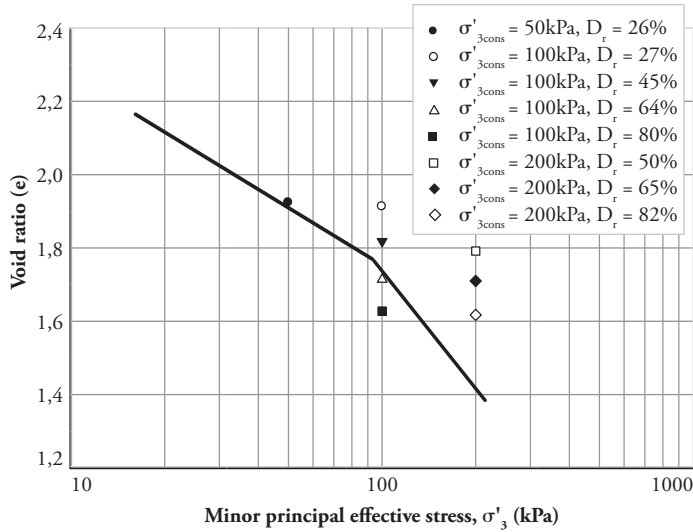


Figure 4. Critical state line (CSL) for the Cabo Rojo calcareous sands.

Cyclic triaxial testing procedure used to assess liquefaction resistance

The liquefaction resistance for both test sands was evaluated by means of consolidated undrained cyclic triaxial tests, which were carried out in general accordance with the procedure described in ASTM Standard D5311 (ASTM 2004). A cyclic triaxial system (Geocomp Corp) was used for the cyclic triaxial tests. Figure 5 shows a photo of the cyclic triaxial equipment used in this research; it shows a loading frame with a hydraulic actuator (LoadTrac II unit), two pressure/volume control units (FlowTrac II) and a PC-based data-acquisition (DAQ) system.

Cyclic triaxial test specimens were prepared using the “moist tamping” technique using five layers and the under-compaction method suggested by Ladd (1976). Prepared samples were about 102 mm high, having 51 mm diameter. The moist tamping technique was carried out with 4% to 25% moisture content for Cabo Rojo calcareous sand and 2% to 8% for Ottawa silica sand. Lower moisture content values were used to produce looser specimens for both test sands while higher moisture content values were used to prepare the denser samples. Relative densities ranged from 20% to 78%. These relative densities corresponded to compacted samples prior to consolidation.

Samples were saturated until greater than 0.95 Skempton B-values were achieved (Skempton, 1954). After saturation, samples were isotropically consolidated at three different effective stress levels (50, 100 and 200 kPa). The soil samples underwent densification during isotropic consolidation, resulting in 26% to 83% final relative density. Specimens were allowed to stabilise once consolidation stress had been reached for at least 30 minutes prior to beginning the cyclic loading phase. The isotropically-consolidated samples were subjected to stress-controlled cyclic triaxial tests at 1 Hz frequency.

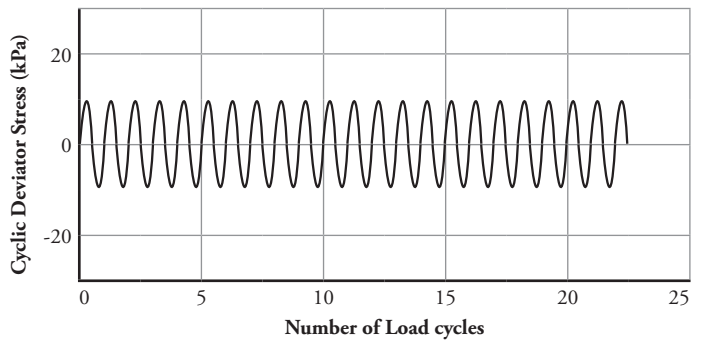
Results and Discussion

Figure 6 shows a typical set of results from this research for a CIU cyclic triaxial tests data regarding on an Ottawa sand sample; this figure shows three plots representing deviator stress, excess pore pressure, and axial strain measurement as a function of number of load cycles. Initial deviator stress (before the cyclic loading) was zero for the isotropically consolidated tests presented here.

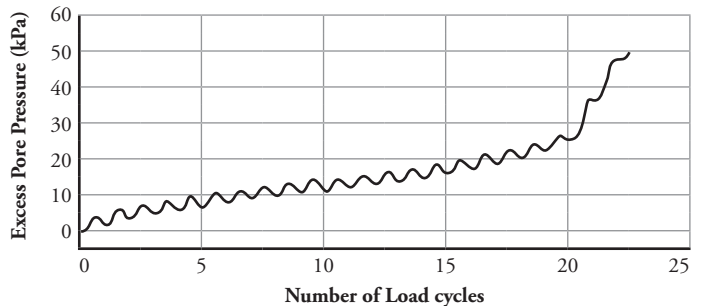
Deviator stress was cycled $\pm \sigma_d$ once a second (1 Hz frequency) in sinusoidal form during cyclic loading (Figure 6a). Two important things occurred to samples during undrained cyclic loading: 1) excess pore pressure



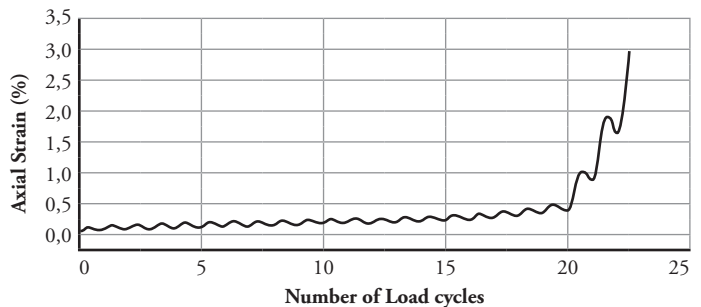
Figure 5. Cyclic triaxial system equipment.



(a) Deviator Stress vs Load Cycle



(b) Excess Pore Pressure vs Load Cycle



(c) Axial Strain vs Load Cycle

Figure 6. An example of test results for an isotropically-consolidated undrained cyclic triaxial test on a reconstituted Ottawa silica sand sample tested at CSR=0.10, σ'_{3cons} =50 kPa, and 1Hz.

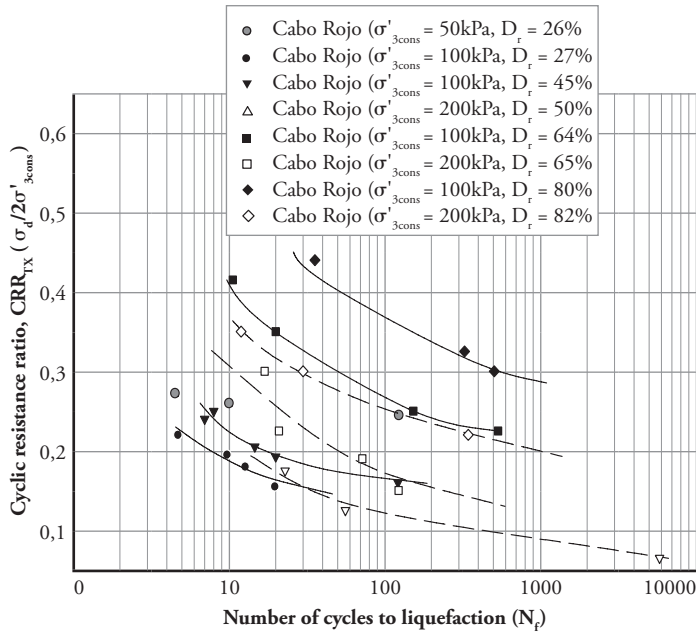


Figure 7. Cyclic resistance curves for Cabo Rojo calcareous sands

started to increase and, as load cycles increased, it approached the consolidation effective stress value (liquefaction is often defined as the condition when excess pore water pressure first equals initial consolidation effective stress, as in Figure 6b) and, II) axial strain was low in the sample at the beginning but then started to increase rapidly after some load cycles (indicating the initiation of liquefaction, see Figure 6c).

The results are presented here in terms of the number of load cycles to liquefaction in response to the cyclic stress ratio (CSR). However, since these curves represent the ability of the soil to resist liquefaction, these curves are often called cyclic resistance ratio (CRR) curves to differentiate them from seismic application on a soil layer, expressed in terms of cyclic stress ratio (CSR) induced by an earthquake.

The CRR for cyclic triaxial tests is defined as the ratio between maximum applied cyclic shear stress and effective consolidation stress, as follows:

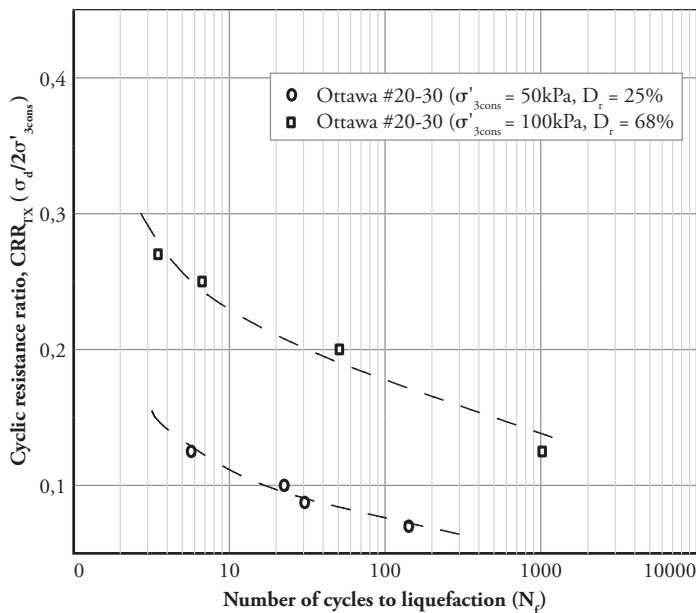


Figure 8. Cyclic resistance curves for Ottawa silica sands.

$$CRR_{TX} = \frac{\sigma_d}{2\sigma'_{3cons}} \quad (1)$$

Three to five cyclic triaxial tests were performed at different CRR_{TX} levels for each relative density and effective consolidation stress level. The number of cycles required to produce liquefaction in the sample was recorded for each CRR_{TX} level. Subscript (TX) mean that CRR was based on cyclic triaxial tests and not on field estimates based on correlations (as in Figure 1). Cyclic liquefaction was considered to have occurred when zero effective stress was reached (i.e. excess pore pressure equalled the consolidation effective stress). The systematic test programme used (involving samples of each sand type) led to obtaining CRR curves for different relative densities and effective consolidation stress levels.

Figure 7 summarises the CRR curves obtained for the Cabo Rojo calcareous sand. These curves represent eight test conditions in terms of relative density and consolidation effective stress, six of which (Figure 4) were on the contractive side of the CSL before cyclic loading. For comparison purposes, Figure 8 shows CRR curves obtained from Ottawa silica sand samples prepared and tested in similar conditions.

Comparing CRR curves for Cabo Rojo calcareous and Ottawa silica sand

Figure 9 compares the liquefaction resistance of Cabo Rojo calcareous sand and Ottawa silica sand for samples prepared in loose state (D_r : 23%–27%) and isotropically-consolidated at 50 kPa effective stress. A similar comparison is presented in Figure 10 for medium to dense state reconstituted samples (D_r : 64%–68%) consolidated at 100 kPa effective stress. Figures 9 and 10 show that Cabo Rojo calcareous sands had much higher liquefaction resistance than Ottawa silica sand, for samples prepared and tested at similar relative densities and effective consolidation stresses.

Excess pore pressure generation

Figure 11 summarises the excess pore pressure produced during triaxial test undrained cyclic loading phase, showing excess pore pressure generation curves for loose state (D_r : 23%–27%) for both test sands consolidated at 50 kPa effective stress.

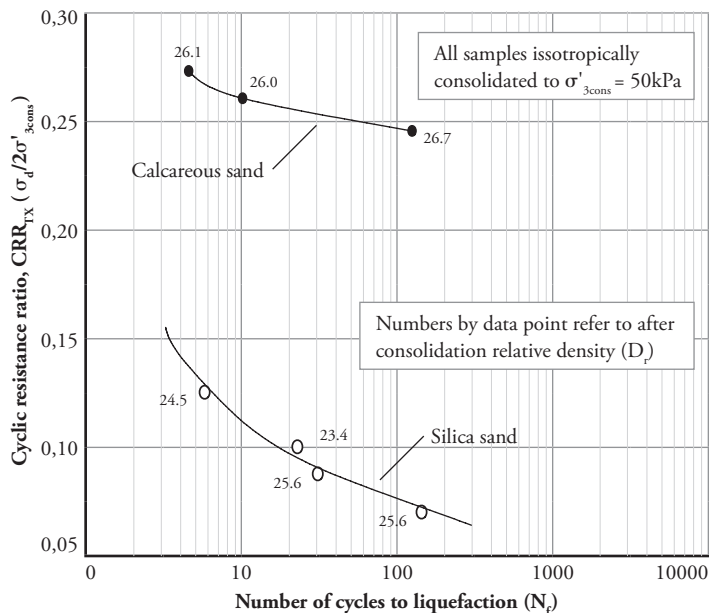


Figure 9. Cyclic resistance curves for loose relative density Cabo Rojo and Ottawa sand.

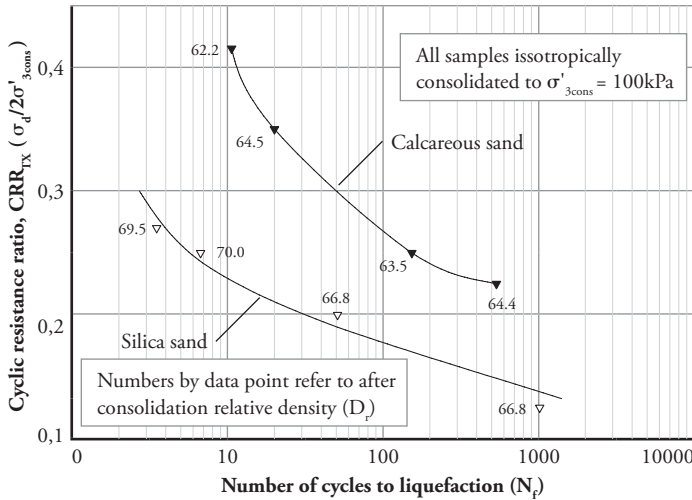


Figure 10. Cyclic resistance curves for medium to dense relative density Cabo Rojo and Ottawa sand.

Figure 12 gives a similar comparison for medium to dense state samples (D_r : 64%–68%), for both test sands consolidated at 100 kPa.

Figures 11 and 12 present normalised residual excess pore pressure (Δu_{res}) regarding consolidation stress (σ'_{3cons}) as a function of the normalised number of cycles for reaching liquefaction (i.e. N/N_f). Residual excess pore pressure (Δu_{res}) was defined as excess pore pressure value when deviator stress was zero during each load cycle (Seed & Lee, 1966). Figures 11 and 12 highlight differences found regarding excess pore pressure generation characteristics between Cabo Rojo calcareous sand and Ottawa silica sand. Calcareous sand developed larger excess pore pressures than the silica sand during the earlier stages of the cyclic loading phase. Calcareous sands had greater fluctuations of excess pore pressures between loading cycles, suggesting some sort of stress relaxation between loading cycles. Silica sands had slow, gradual excess pore pressure generation during the initial test cyclic loading phase and very small pore pressure fluctuations between loading cycles.

Another important difference was that silica sands typically showed a sudden or abrupt increase in excess pore pressure towards the end of the tests (i.e. as the sample approached liquefaction) while the calcareous sands showed a more gradual or incremental increase in excess pore pressure as it reached liquefaction.

The large fluctuations in excess pore pressure exhibited by calcareous sands during loading cycles could have been due to particle rearrangement arising from the characteristics concerning contact areas between

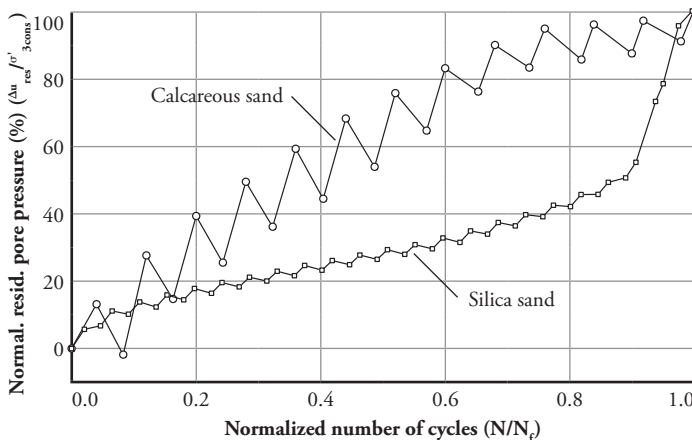


Figure 11. Excess pore pressure generation curves for loose state Cabo Rojo and Ottawa sands, isotropically-consolidated at 50 kPa effective stress.

grains, including unique particle shapes, surface roughness, intra-grain porosity, etc.

The occurrence of large pore pressure relaxation between loading cycles could contribute towards the greater cyclic resistance exhibited by the Cabo Rojo calcareous sands compared to Ottawa silica sand. Cabo Rojo sand excess pore pressure generation characteristics were similar to that reported by Morioka & Nicholson (2000) and Ross & Nicholson (1995) for two calcareous sands from Hawaii.

Development of axial strains

Samples in cyclic triaxial testing experienced a marked increase in accumulated axial strain when approaching liquefaction state; this is due to large soil stiffness losses as the effective stress in the sample decreases and eventually reaches zero at cyclic liquefaction.

How axial strains are accumulated in a sample to reach liquefaction depended largely on the initial position of the sample regarding the CSL (i.e. if the initial state before loading was contractile or dilatant). The individual characteristics of the sand grains are another important factor on how permanent axial strains are developed and accumulated. Similar to the finding for excess pore pressures, the unique properties of calcareous sands had a great influence on how axial strains were developed during cyclic triaxial tests.

Figure 13 illustrates simultaneously the axial strain accumulation of calcareous and silica sand to loose state samples ($D_r = 23\%-27\%$) consolidated under an effective stress of 50 kPa. A similar comparison is presented in Figure 14 for samples in medium to dense state ($D_r = 64\%-68\%$) consolidated to 100 kPa. It may be noted in these figures that calcareous sand experienced an increase in axial strain amplitude since the start of cyclic loading, gradually increasing until liquefaction. Calcareous sands underwent no dramatic increase in axial deformation, even to reach liquefaction state. Moreover, silica sands were deformed very little during the cyclic test, but experienced a sudden increase in axial strain just before liquefaction, when pore pressure increased. Axial strain amplitude for both sands increased with increasing relative density.

Summary and Conclusions

This paper has presented a summary of an experimental study for assessing the liquefaction resistance of uncemented calcareous sands from Cabo Rojo in south-western Puerto Rico. The cyclic triaxial tests revealed important differences between the response of calcareous sands and samples prepared with silica sand tested under similar conditions. The calcareous

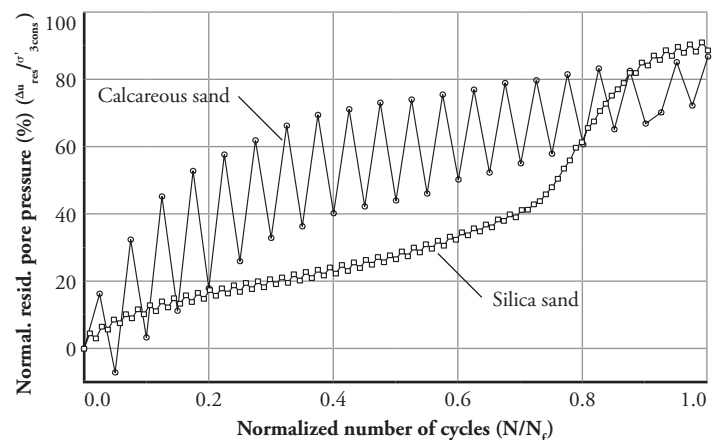


Figure 12. Excess pore pressure generation curves for medium to dense state Cabo Rojo and Ottawa sands, isotropically-consolidated at 100 kPa effective stress.

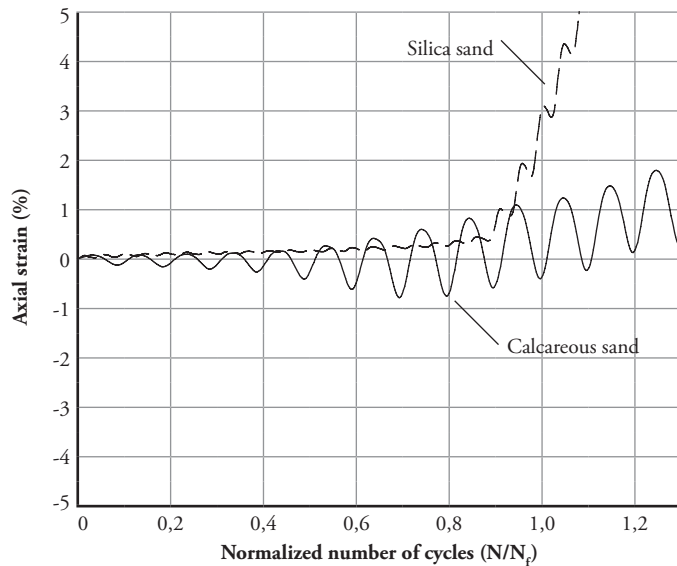


Figure 13. Development of axial strains for loose state Cabo Rojo and Ottawa sands, isotropically-consolidated at 50 kPa effective stress.

ous sand had greater liquefaction resistance than Ottawa silica sand tested at similar relative densities and effective consolidation stress levels.

The Cabo Rojo calcareous sand also had unique characteristics regarding their excess pore pressure generation curves which showed large fluctuations between loading cycles. These fluctuations could be attributed to stress relaxations due to the unique characteristics of this sand, such as particle shape, roughness and intra-particle porosity resulting in important differences in the characteristics of particle contact in samples of this sand compared to Ottawa silica sand samples.

In terms of axial strain development, calcareous sand also had a unique response under cyclic triaxial loading; axial strain gradually increased until cyclic liquefaction was reached. Whereas for the Ottawa silica sand a sudden marked increase in axial strains was consistently observed just before samples reaching a state of cyclic liquefaction.

It may thus be affirmed that based on the important differences observed in terms of cyclic triaxial testing, between the Cabo Rojo calcareous sands and the quartzitic terrigenous Ottawa sands, conventional empirical in-situ based liquefaction methods (e.g. the SPT based simplified liquefaction method) not provide good support for evaluating liquefaction resistance for calcareous sands, due to their particular mineralogy, particle characteristics and associated geotechnical behaviour.

Acknowledgements

The authors would like to acknowledge the financial support provided by the Puerto Rico Strong Motion Program and the PR Sea Grant which partially funded the assistantship for the first author. Additional funding for this research project came from a NEHRP-USGS project.

References

- ASTM (2004). ASTM D 5311 – 92: Standard Test Method for Load Controlled Cyclic Triaxial Strength of Soil: ASTM Standard, American Society for Testing and Materials, ASTM International, USA.
- Been, K., and Jefferies, M. G.. A state parameter for sands, *Geotechnique*, 35, no. 2, 95-112.
- Cataño, J., and Pando, M.A. (2010). Static and dynamic properties of a calcareous sand from southwest Puerto Rico, *GeoFlorida 2010*, American Society of civil Engineers (ASCE), West Palm Beach, Florida, USA, February, 842-851.

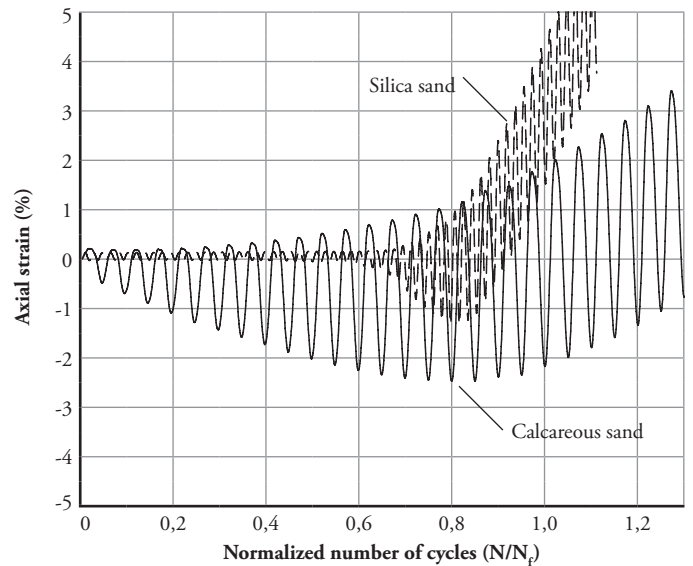


Figure 14. Development of axial strains for medium to dense state Cabo Rojo and Ottawa sands, isotropically-consolidated at 100 kPa effective stress.

- Chaney, R. C., Slonim, S. M., and Slonim, S. S. (1982). Determination of calcium carbonate content in soils, geotechnical properties, behavior and performance of calcareous soils, *ASTM Special Technical Publication 777*, 3-15.
- Idriss, I.M., and Boulanger, R.W. (2010). SPT-based liquefaction triggering procedures, Report No. UCD/CGM-10/02, Center for Geotechnical Modeling, University of California at Davis, California, USA.
- Ladd, R.S. (1976). Preparing test specimens using undercompaction, *Geotechnical Testing Journal*, GTJODJ. 1, no. 1, 16-23.
- Morelock, J., and Ramirez, W. (2004). Marine Sediments, *Marine Geology*, http://geology.uprm.edu/Morelock/GEOLOCN_/sedimt.htm (last accessed February 2006).
- Morioka, B. T., and Nicholson, P. G. (2000). Evaluation of the liquefaction potential of calcareous sand, 10th International Offshore and Polar Engineering Conference, Seattle, Washington, USA, June, 494-500.
- Morse, J. W., and Mackenzie, F. T. (1990). *Geochemistry of Sedimentary Carbonates*, Elsevier Science Publishers B. V., Amsterdam, Holland, 707 pp.
- NRC (1985). *Liquefaction of Soils during Earthquakes*. National Academic Press, Washington, D.C., USA, 240 pp.
- Pando, M., and Robertson, P.K. (1995). Evaluation of shear stress reversal due to earthquake loading for sloping ground, 48th Canadian Geotechnical Conference, Vancouver, B.C., Canada, September, 955-962.
- Robertson, P.K. (1994). Suggested terminology for liquefaction, 47th Canadian Geotechnical Conference, Halifax, Canada, September, 277-286.
- Robertson, P. K., and Wride, C.E. (1998). Evaluating cyclic liquefaction potential using the cone penetration test, *Canadian Geotechnical Journal*, 35, no. 3, 442-459.
- Ross, M. S., and Nicholson, P. G. (1995). Liquefaction potential and cyclic loading response of Calcareous Soils, Research Report UHM/CE/95-05, University of Hawaii, Manoa, Hawaii, USA.
- Santamarina, J. C. and Cho, G. C. (2001). Determination of critical state parameters in sandy soils — simple procedure, *Geotechnical Testing Journal*, GTJODJ. 24, no. 2, 185-192.
- Seed, H.B. (1979). Soil liquefaction and cyclic mobility evaluation for level ground during earthquakes, *Journal of the Geotechnical Engineering Division ASCE*, 97, no. SM9, 1249-1273.
- Seed, H. B., and Idriss, I. M. (1971). Simplified procedure for evaluating soil liquefaction Potential, *Journal of the Soil Mechanics and Foundation Division*, 97, no. 9, 1249-1273.

- Seed, H.B., and Idriss, I.M. (1982). Ground Motions and Soil Liquefaction during Earthquakes, Earthquake Engineering Research Institute, Berkeley, CA, USA, 134 pp.
- Seed, H. B., and Lee, K. L. (1966). Liquefaction of saturated sands during cyclic loading, *Journal of the Soil Mechanics and Foundation Division*. 92, no. 3, 25-58.
- Silva, A.J. (1974). Marine geomechanics: an overview and projections. In: *Deep-sea Sediments: Physical and Mechanical Properties*: Ed. A.L. Inderbitzen. New York: Plenum Press, 45-76.
- Skempton, A. W. (1954). The pore pressure coefficients A and B, *Geotechnique*. 4, 143-147.
- Yoshimi, Y., Richart, F.E., Prakash, S., Balkan, D.D., and Llyichev, V.A. (1977). Soil dynamics and its application to foundation engineering, 9th International Conference on Soil and Mechanics and Foundation Engineering, Tokyo, Japan, July, 605-650.
- Youd, T.L., Idriss, I.M., Andrus, R.D., Arango, I., Castro, G., Christian, J.T., Dobry, R., Finn, W.D.L., Harder, L.F., Hynes, M.E., Ishihara, K., Koester, J., Liao, S., Marcuson III, W.F., Martin, G.R., Mitchell, J.K., Moriwaki, Y., Power, M.S., Robertson, P.K., Seed, R., and Stokoe, K.H. (2001), Liquefaction resistance of soils, Summary Report from the 1996 NCEER and 1998 NCEER/NSF Workshops on Evaluation of Liquefaction Resistance of Soils, *Journal of Geotechnical and Geoenvironmental Engineering*, ASCE, 127, no. 10, 817-833.